

Solvent Dependence of Polystyrene Local Segmental Dynamics in Dilute Solution by Spin-Label X-Band ESR

Jan Pilar* and Jiří Labský

Institute of Macromolecular Chemistry, Academy of Sciences of the Czech Republic,
162 06 Prague, Czech Republic

Received September 24, 2002; Revised Manuscript Received December 11, 2002

ABSTRACT: A styrene copolymer with methacrylic acid containing less than 5 mol % of spin-labeled methacrylic acid chain units distributed randomly along the polymer main chain (SL–ST–MA) was synthesized. ESR spectra of the copolymer were measured at X-band (9 GHz) in dilute solutions (ca. 1 wt %) over a broad temperature range in four solvents differing in thermodynamic quality, viscosity, and activation energy of viscous flow. Temperature dependences of the parameter R_s characterizing local dynamics in polystyrene chains and of other parameters characterizing dynamics in the copolymer were determined by fitting experimental ESR spectra to the MOMD model. Unlike so far published conclusions, the data show that the copolymer in the solvents used— Θ solvent dioctyl phthalate (DOP), marginal solvent dibutyl phthalate (DBP), and good solvents toluene (TOL) and dimethylformamide (DMF)—exhibits non-Kramers behavior characterized by the parameter $\alpha = 0.73 \pm 0.02$ and by the height of the potential barrier for local conformational transitions $E_a = 10.5 \pm 0.6$ kJ/mol.

Introduction

Study of local segmental dynamics of polymers plays a significant role in understanding structure–property relationships shown by different polymers. The relationships represent an important subject in polymer research. It is useful to study local chain motions of an isolated chain in dilute solutions before chain–chain interactions are taken into account. Dynamics on the length scale of a few monomer units depends strongly on the conformation of the polymer chain in dilute solution resulting, among others, from the polymer–solvent interaction. In recent years a great deal of effort has been devoted to understanding the local dynamics of polymers by measuring the correlation time, τ_c , for segmental rotational diffusion of polymers in dilute solution. Measurement of the fluorescence depolarization of the anthracene chromophore bonded inside the main chain^{1–14} and measurement of ¹³C NMR relaxation times and NOE values^{15–23} have mainly been used for this purpose. Computer simulation studies have been performed as well.^{24–26} It was shown that Kramers's theory²⁷ in the high-friction limit resulting in eq 1 shown below with $\alpha = 1$ cannot accurately describe the segmental dynamics of a synthetic polymer in dilute solutions. For some polymers in solvents with high viscosity and large activation energy of viscosity, the theory yields nonphysical negative values for the height of the potential barrier for segmental rotation.⁴ That is, the prediction that the experimental correlation times should scale linearly with viscosity at constant temperature is generally not fulfilled. A power law relationship between τ_c and the solvent viscosity η with an exponent $0 \leq \alpha \leq 1$ was suggested¹⁸ on the basis of papers published by Fleming and co-workers²⁸

$$\tau_c = A[\eta(T)]^\alpha \exp(E_a/RT) = A' \exp(E_{\text{exp}}/RT),$$

$$E_{\text{exp}} = E_a + \alpha E_\eta \quad (1)$$

where

$$\eta(T) = \eta_0 \exp(E_\eta/RT) \quad (2)$$

providing that the temperature dependence of viscosity exhibits Arrhenius behavior in the temperature range investigated, and E_η is the activation energy of viscous flow of the solvent. The prefactor A is independent of temperature and viscosity; E_{exp} is the activation energy determined from an Arrhenius plot of a parameter characterizing local segmental mobility (e.g., τ_c). Also, A' is independent of temperature, E_a is the height of the potential barrier for local segmental motions, T is the absolute temperature, and R is the gas constant. The exponent α is assumed to depend on the moment of inertia and size of the isomerizing unit and on the curvature at the top of the potential barrier. A larger size, a larger moment of inertia, or a lower barrier prolongs the time required to get across the barrier and thereby leads to a larger value of α . When this time is sufficiently long, then the high-frequency behavior of friction is less significant, and behavior close to Kramers's high-friction limit should be observed. The value of the exponent α is expected to vary from polymer to polymer. The height of the intramolecular potential barrier E_a should not depend on the solvent viscosity, but it may vary with conformation of the polymer in solution. It follows that it should be solvent-independent for all good nonpolar solvents for a particular polymer but may change in bad solvents and in Θ solutions.¹⁸

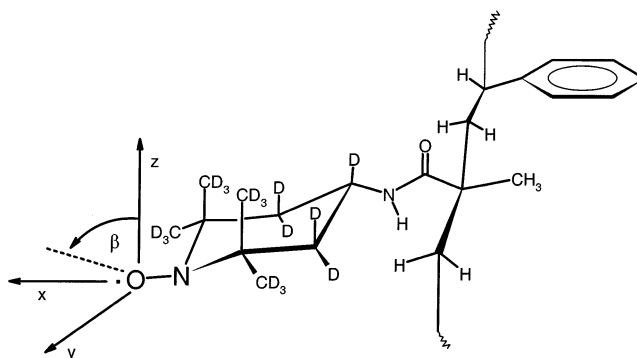
For polyisoprene the values $E_a = 13 \pm 2$ kJ/mol and $\alpha = 0.41 \pm 0.02$ were found by ¹³C NMR¹⁸ and the values $E_a = 10 \pm 1$ kJ/mol and $\alpha = 0.75 \pm 0.06$ by fluorescence depolarization.⁴ The difference in E_a is small and may be related to a modification of the potential barrier by the presence of the anthracene chromophore, because the fluorescence measurement senses the chain motion in the vicinity of anthracene. A larger size of the isomerizing unit and a larger moment of inertia due to the presence of the anthracene chromophore in the labeled chain would explain the

* Corresponding author. E-mail: pilar@imc.cas.cz.

higher α value determined by fluorescence depolarization. ^{13}C NMR study of segmental mobility of poly(1-naphthylmethyl acrylate) (PNMA) in chlorinated solvents (1,1,2,2-tetrachloroethane- d_2 , pentachloroethane, and CDCl_3) has shown²¹ that Kramers' theory is correct for the polymer system in the range of viscosities studied ($\alpha = 1.07$) and provides $E_a = 11.3$ kJ/mol for the segmental PNMA dynamics. Kramers' theory has also succeeded in explaining results of ^{13}C NMR study of poly(*N*-vinylcarbazole) (PNVC) in five solvents covering viscosities differing by a factor of 5, and it has afforded $E_a = 9.1 \pm 0.3$ kJ/mol for PNVC chain local dynamics.²³ A similar study of poly(vinyl chloride) (PVC) in three solvents (chloroform, dioxane, and dimethyl sulfoxide) has revealed²² deviation of this polymer system from Kramers' theory characterized by $\alpha = 0.6$ and $E_a = 19.5 \pm 2.5$ kJ/mol. A fluorescence depolarization study of local chain dynamics of poly(oxyethylene) (POE) in only two solvents (dimethylformamide and cyclohexane) has shown non-Kramers' behavior in this case characterized by $\alpha = 0.69$ and $E_a = 5$ kJ/mol.¹⁰

The temperature dependence of the correlation times for the rotational diffusion of the anthracene chromophore bonded inside the polystyrene main chain in various solvents measured by fluorescence depolarization resulted in the value $\alpha = 0.90 \pm 0.05$, which was considered a reasonable agreement with Kramers' theory.² The larger α observed for labeled polystyrene in comparison with labeled polyisoprene was rationalized by the presence of the bulky benzene rings in polystyrene. The height of the potential barrier $E_a = 11 \pm 3$ kJ/mol has been found for polystyrene in good solvents and higher values in Θ solutions ($E_a = 21 \pm 2$ kJ/mol in cyclohexane). In all earlier papers dealing with polystyrene local dynamics, the data were analyzed in the frame of Kramers' theory. Heatley and Wood¹⁶ measured ^1H spin-lattice relaxation times for polystyrene protons in 5% solutions in four solvents using NMR. They determined activation energy for correlation time characterizing conformational jumps of polystyrene chains and found the potential barrier height $E_a = 11$ – 16 kJ/mol for polystyrene in chlorinated solvents (CDCl_3 , CCl_4 , and hexachlorobutadiene) and the value $E_a = 19 \pm 5$ kJ/mol for polystyrene in 90/10 (vol) solution of cyclohexane- d_{12} and toluene- d_8 , which is a Θ solvent for polystyrene at 15 °C. Gronski et al.¹⁷ performed ^{13}C spin-lattice relaxation and nuclear Overhauser effect measurements of 1% solutions of ^{13}C -enriched polystyrene and found activation energies for three bond rearrangements. They determined heights of potential barriers for polystyrene conformational transitions: $E_a = 15$ and 10.5 kJ/mol for ^{13}C -enriched polystyrene in benzene and toluene solutions, respectively. Yokotsuka et al.⁶ measured the mean relaxation time related to local conformational transitions of the anthracene-labeled polystyrene by the fluorescence depolarization method. They found heights of potential barriers $E_a = 6.3$, 6.7, 2.9, 3.3, and -8.0 kJ/mol in butyl acetate, cyclohexane, dioxane, cyclohexanone, and more viscous glycerol tripropionate, respectively, using the original Kramers' equation. When applying the generalized equation combining both high- and low-friction limits suggested by Helfand,²⁹ they found heights $E_a = 6.7$, 7.1, 5.0, 5.0, and 8.0 kJ/mol in the mentioned solvents. Ono et al.^{8,10} used the same technique and determined heights of potential barriers for local conformational transitions in polystyrene chain in various solvents,

Chart 1



including Θ solvents. They found $E_a = 5.9$, 7.5, and 10.9 kJ/mol in toluene, butyl acetate, and Θ solvent cyclohexane, respectively, using the classic Kramers' approach. Horinaka et al.¹³ studied the influence of a fluorescent probe on the local relaxation times and their dependence on molecular weight and tacticity of the polystyrene used. They found $E_a = 7.1$ kJ/mol for $M_w > 10^4$ when applying the classic Kramers' approach.

Data characterizing local rotational dynamics of polymer chains in dilute solutions can be obtained by ESR of dilute solutions of spin-labeled polymers as well.^{30–33} Parameters characterizing rotational diffusion of nitroxide spin-labels embedded in a particular system may be determined by analysis of their ESR spectra.³⁴ Rotational diffusion of a nitroxide spin-label, which is attached to chain segments of a polymer at randomly distributed sites, has been approximated by superposition of isotropic rotational diffusion of the polymer chain segment characterized by rotational diffusion coefficient R_s and internal rotation of the spin-label about the tether through which it is attached to the polymer chain segment characterized by rotational diffusion coefficient R_i .^{30–33} The contribution of rotational diffusion of the polymer coil as a whole has been neglected for the high-molecular-weight polymers. When the spin-label is attached to the polymer chain via a short tether containing only a single bond through which conformational transitions of the tether can occur, then the axis of internal rotation of the spin-label should be identical to this bond axis. This approximate model gives rise to axially symmetric rotational diffusion with two components of the rotational tensor, $R_{\text{prp}} = R_s$ and $R_{\text{pll}} = R_s + R_i$. In addition, the axis of internal rotation can be tilted relative to the z axis of the nitroxide axis system, which is specified by angle β . This is shown in Chart 1 for the 2,2,6,6-tetramethylpiperidin-1-yloxy type spin-label. In this case the tether involves three single bonds (C–CO, CO–NH, and NH–SL). Given that the second bond, which is a peptide bond, is normally fixed, and there are steric constraints on the first bond, the only bond through which conformational changes of the tether occur is the NH–SL bond. At the X-band ESR frequency (9 GHz), rotational dynamics in most fluids is usually sufficiently fast, i.e., $\tau_R \Delta\omega \ll 1$ (where the correlation time $\tau_R = (6)^{-1}(R_{\text{prp}}^2 R_{\text{pll}})^{-1/3}$ and $\Delta\omega$ is a measure of the magnitude of the orientation-dependent part of the spin-Hamiltonian), and such motions fall within the motional narrowing regime. In such cases the ESR spectrum is a simple superposition of Lorentzian lines whose widths cannot be fully and unambiguously related to parameters characterizing the nitroxide rotational diffusion by the motional narrowing theory without additional assumptions on the motion. For

slower motions, in more viscous media, where $\tau_R \Delta\omega \geq 1$, the ESR spectrum depends more dramatically on the combined influences of molecular motion and magnetic interactions. Thus, the slow-motional ESR line shapes, in principle, provide a more detailed picture of rotational dynamics when compared with motionally narrowed line shapes. These slow-motional line shapes can be fully analyzed using a theoretical approach based on numerical solution of the stochastic Liouville equation.^{34,35}

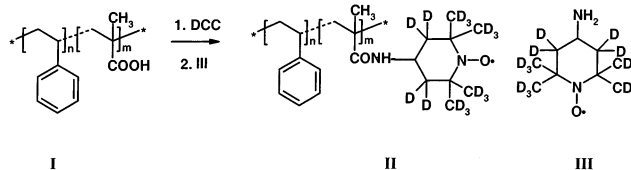
In their pioneering X-band ESR study of spin-labeled polymers dynamics, Bullock et al.³⁶ used polystyrene spin-labeled by attachment of *tert*-butyl nitroxide to the para positions of polystyrene benzene rings at randomly distributed sites. They characterized the spin-label dynamics in dilute (1 wt %) solutions by a single isotropic correlation time calculated in a simple way using motional narrowing theory and widths and amplitudes of the three constituent Lorentzian lines of the spectrum. From the temperature dependence of experimental correlation times they estimated the barriers heights in polystyrene $E_a = E_{\text{exp}} - E_\eta = 8.8$ kJ/mol in toluene and 1-chloronaphthalene and at least 12.6 kJ/mol for cyclohexane, when applying the classic Kramers' approach.

In the recent paper,³³ we have presented results of the multifrequency ESR study (X-band 9.5 and 250 GHz) of polystyrene segmental dynamics in dilute toluene solutions. We have used a copolymer of styrene with spin-labeled acrylic acid (SL-ST-AA) and spectral analysis based on the stochastic Liouville equation.^{34,35} We have shown that the MOMD (microscopic order with macroscopic disorder) model introduced by Meirovitch et al.^{34,37} is very successful in analyzing ESR line shapes of spin-labeled polymers. This model allows for constraints in the above-mentioned motions. More precisely, we regard the polymer chain segmental motion sensed by the tethered nitroxide, i.e., the wobbling motion of the effective axis of internal rotation, as constrained by an orienting potential typically given by

$$-U(\theta, \varphi)/kT = \sum_{L=2,4} \{ c_0^L D_{00}^L(\theta, \varphi) + c_2^L [D_{02}^L(\theta, \varphi) + D_{-2}^L(\theta, \varphi)] \} \quad (3)$$

where the c_0^L terms refer to strength and shape of the restricting potential for the wobbling motion and the c_2^L to its asymmetry and $D_{0k}^L(\theta, \varphi)$ are Wigner rotation matrix elements. The angles θ and φ are respectively the polar and azimuthal angles for a unit vector along the preferred orientation for the internal axis in the frame of the polymer with respect to the instantaneous orientation of the tethered nitroxide expressed in the principal axes of its rotational diffusion. Although we have found a reasonable agreement between the results obtained at 9 and 250 GHz, there were systematic discrepancies such that the orienting potentials obtained from the 250 GHz spectra were about twice (or more) higher than those from the 9 GHz spectra, and the rotational diffusion tensor components from the 250 GHz spectra were at least twice higher than those from the 9 GHz spectra. This implies a greater sensitivity of the 9 GHz spectra to the slower tumbling motions. For the faster "time scale" of the 250 GHz spectra, such motions are likely "frozen out", consistent with the MOMD model. Nevertheless, the results at both frequencies yielded a common activation energy, $E_{\text{exp}} =$

Chart 2



20.7 ± 1.5 kJ/mol, which, when corrected for the viscous flow contribution according to the classic Kramers' theory, yielded $E_a = 11.9 \pm 1.5$ kJ/mol.

In the present paper we describe results obtained when studying the solvent dependence of polystyrene local segmental dynamics using the ESR spin-label technique regarding its possible non-Kramers' behavior. This technique makes possible extraction of information on the polymer chain local dynamics from the data characterizing rotational dynamics of the nitroxide spin-label the dimensions of which are similar to the dimensions of the styrene moiety. Geometry and volumes of isomerizing units in the vicinity of the spin-label "reporter" group in the case of spin-labeled polystyrene are much less affected by the presence of the label group than in the case of the anthracene chromophore bonded inside the polystyrene chain used in fluorescence depolarization measurements. X-band ESR spectra of dilute solutions of a poly(styrene-*co*-methacrylic acid) random copolymer spin-labeled in methacrylic acid units (SL-ST-MA) in four solvents covering a broad viscosity range and differing in the thermodynamic quality have been measured in a suitable temperature range and analyzed in a similar way as previously.³³

Experimental Section

Synthesis and Characterization of Spin-Labeled Copolymer. Poly(styrene-*co*-methacrylic acid) (ST-MA) (I). A mixture of 10 g of styrene, 0.5 g of methacrylic acid, and 0.001 g of 2,2'-azobis(2-methylpropanonitrile) was bubbled with argon for 10 min, sealed into an ampule, and copolymerized at 60 °C for 10 h (Chart 2). The copolymer was dissolved in 30 mL of dioxane and precipitated into 350 mL of methanol. The carboxyl content 3.5 mol % was found by titration. The mass-average molecular weight, M_w , equal to 3.6×10^5 , was determined by light scattering in dioxane with a modified Sofica 42.000 instrument at 546 nm and 25 °C. Refractive index increments were measured under the same conditions with a Brice-Phoenix BP-2000 V differential refractometer.

Poly(styrene-*co*-(4-methacrylamidoperdeuterio-2,2,6,6-tetra- $[\text{}^2\text{H}_3]$ methyl)(3,3,5,5- $[\text{}^2\text{H}_4]$ piperidin-1-yloxy)) (SL-ST-MA) (II). To a solution of 2 g of copolymer ST-MA in a benzene-dioxane mixture (1:1, 50 mL) cooled to 5 °C were added dicyclohexylcarbodiimide (Fluka, 1 g) and 4-amino-2,2,6,6-tetra- $[\text{}^2\text{H}_3]$ -methyl-3,3,5,5- $[\text{}^2\text{H}_4]$ piperidin-1-yloxy (III) (0.1 g). The reaction mixture was concentrated to approximately 10 mL after standing for 48 h at room temperature, and the spin-labeled copolymer (SL-ST-MA) (II) was precipitated repeatedly into methanol until the free spin-label completely disappeared in the ESR spectrum. The perdeuterated spin-label (III) was synthesized as described previously.³⁸ If not specified, all chemicals are from Aldrich and were used without further purification.

ESR Measurements. X-band ESR spectra have been recorded over a suitable temperature range at 110–400 K with a JEOL-PE-3X spectrometer interfaced to the PC Pentium 90 MHz. Dilute solutions of the copolymer (approximately 1 wt %) of the spin-labeled copolymer in the solvents used were bubbled with nitrogen and filled into quartz capillaries. The measurements were performed with 100 kHz magnetic field

modulation at a microwave output of 2 mW. The cavity temperature was stabilized with a JES-VT-3A temperature controller to ± 0.5 K and measured with a platinum thermometer GMH 2000. The magnetic field was measured with a MJ-110R NMR magnetometer (Radiopan Poznań). The g factors were measured relative to the fourth line of the Mn^{2+} cation ($g = 1.981$) in the MgO ESR marker.

Analysis of ESR Spectra. Both rigid-limit and slow-motional ESR spectra were calculated utilizing the spectral simulation method based on the stochastic Liouville equation.³⁴ The simulated spectra were fitted to the experimental ones using a PC version of the NLSL program³⁵ based on a modified Levenberg–Marquart minimization algorithm which iterates the simulations until a minimum least-squares fit to experiment is reached. This provides optimum values for the fitted parameters as well as estimates of error.

In the first step of the analysis, the **A** and **g** tensors of the spin-label attached to the SL–ST–MA copolymer in the particular solvent were determined by analyzing rigid-limit spectra of the sample. Rotational diffusion tensor components have been set at very low values and **A** and **g** tensor components, and inhomogeneous Lorentzian and/or Gaussian broadening have been used as the fitted parameters during the analysis. The presence of ordering potential has not been considered in the case of rigid-limit spectra. The principal axis systems of both tensors were considered identical, and their tensor components were assumed to be independent of the temperature.

The values of the **A** and **g** tensor components were fixed throughout the analysis of slow-motional ESR spectra in the particular solvent. The MOMD model^{34,37} for spin-label rotational diffusion was assumed. In this case fitted parameters include the parallel and perpendicular rotational diffusion coefficients R_{pl} and R_{prp} , the diffusion tilt β , the inhomogeneous Lorentzian broadening, and the parameters c_0' and c_2' characterizing the ordering potential. When all c_0' and c_2' are zero, one then has simple Brownian rotational diffusion. All spectral simulations were performed on a 468 MHz PC equipped with two CELERON processors.

Viscosity of Solvents. According to literature data, the temperature dependence of viscosity of the solvents used cannot be described by a simple function (eq 2) in a broader temperature range. For toluene (TOL), we have used the empirical expressions η [mPa s] = $1895.4 / (112.99 + T[^\circ\text{C}])^{1.6522}$ and $\log \eta$ [mPa s] = $-1.156 - 177.85 / (103.1 - T[\text{K}])$ suggested on the basis of experimental data measured in the ranges 273–380 K³⁹ and 155–288 K,⁴⁰ respectively. The data presented in Figure 1 show that these expressions fit recently published experimental viscosities⁴¹ very well. The temperature dependence of viscosities of some solvents can be described by the Vogel–Fulcher (V–F) expression⁴² $\ln \eta = A + B / (T + C)$. This expression has been fitted to the viscosities measured⁴³ for dibutyl phthalate (DBP) and dioctyl phthalate (DOP) in the temperature range 2–130 °C. The best-fit values of the parameters $A = -2.4617$, $B = 707.86$, $C = 84.543$ and $A = -2.0386$, $B = 572.12$, $C = 94.286$ have been determined⁴³ for DOP and DBP, respectively. Figure 1 shows that the V–F expression with these parameters fits also well other experimental DOP⁴⁴ and DBP^{41,44} viscosities taken from the literature. Berry⁴⁶ found the Θ temperature of the system polystyrene–DOP to be 22 °C; Štěpánek et al.⁴⁷ measured the coil–globule transition in this system using the light scattering technique. DBP has been characterized as marginal (near Θ solvent) for polystyrene.^{48,49} The Θ temperature of the DBP–polystyrene system has been estimated to be -14 °C.⁵⁰ In the case of dimethylformamide (DMF), we have fitted a temperature dependence for published experimental viscosities^{41,45} by the V–F type expression, and the best-fit values for the parameters $A = -4.2426$, $B = 1265.0$, and $C = 14.754$ have been determined. The absence of experimental DMF viscosities measured at temperatures below 263 K decreases the accuracy of the low-temperature part of this fit.

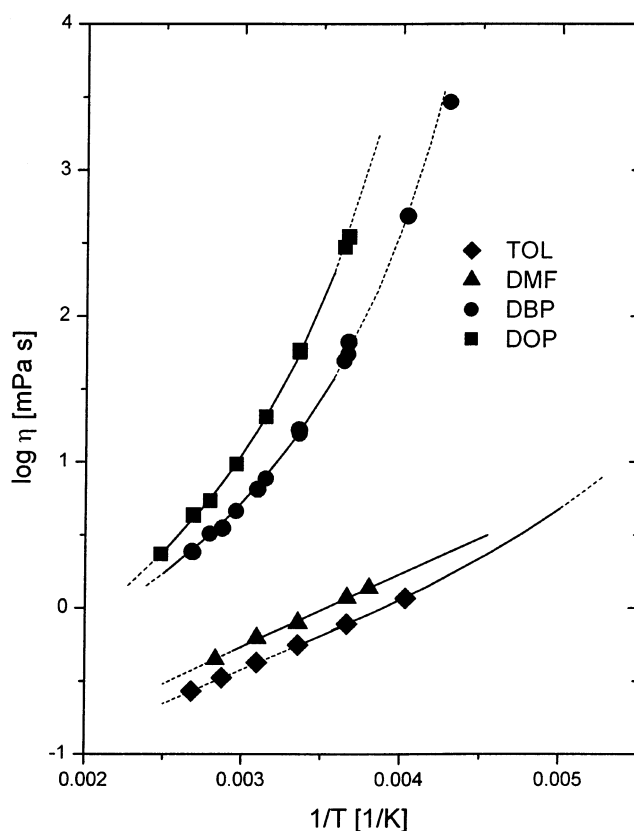


Figure 1. Temperature dependence of solvent viscosities. Literature data for toluene,⁴¹ dimethylformamide,^{41,45} dibutyl phthalate,^{43,44} and dioctyl phthalate^{43,45} and fits calculated using expressions given in the text are presented (solid parts of the curves represent the temperature range studied).

Results and Discussion

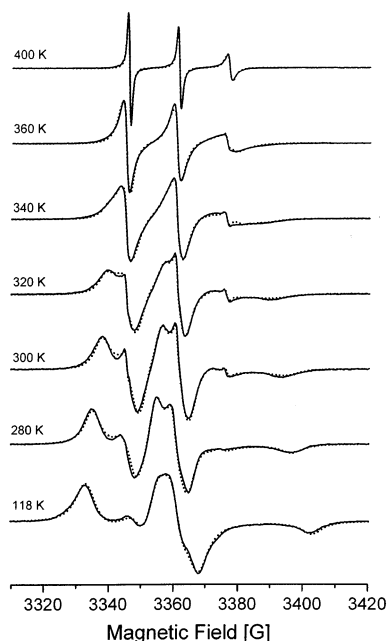
Components of **A** and **g** tensors of the nitroxide spin-label attached to polystyrene chains in the solvents used have been determined in the usual way from rigid-limit ESR spectra of the spin-labeled copolymer measured in frozen solutions at 120 K. The rigid-limit spectra were successfully fitted using the NLSL program and very slow isotropic Brownian rotational diffusion of the spin-label ($R_{\text{prp}} = R_{\text{pl}} = 1 \times 10^3 \text{ s}^{-1}$). The calculations converged very well when using a quite tractable basis set characterized by the parameters³⁵ $\text{lemx} = 40$, $\text{lomx} = 39$, $\text{kmx} = 16$, $\text{mmx} = 2$, and $\text{ipnmx} = 2$. Best fits required axially symmetric Lorentzian inhomogeneous broadening characterized by the parameters w_{prp} and w_{pl} and a Gaussian inhomogeneous broadening characterized by the width parameter gib0 . This corresponds to a combined Lorentzian–Gaussian line shape frequently observed in rigid limit spectra. It should be noted that the line shapes of the well-resolved spectra are very sensitive to the A_{xx} and A_{zz} values but less sensitive to the A_{yy} values. The uncertainty in A_{yy} was resolved by adopting the values calculated from the isotropic nitrogen hyperfine splitting determined from the motionally narrowed three-line spectra. The best fit values of **A** and **g** tensor components and other parameters determined for all four solvents used are presented together with the values for the spin-labeled poly(styrene-*co*-acrylic acid) (SL–ST–AA) copolymer in toluene solvent determined previously³³ in Table 1.

Experimental ESR spectra of the SL–ST–MA copolymer in DOP taken in a suitable temperature range are presented as an example in Figure 2 together with

Table 1. A and g Tensor Components^a for the Nitroxide Spin-Label and Other Parameters Determined by the Analysis of Rigid-Limit ESR Spectra of the Spin-Labeled Poly(styrene-co-methacrylic/acrylic acid) Copolymers (SL-ST-MA/AA) in Indicated Solvents at 120 K

solvent	A_{xx}	A_{yy}	A_{zz}	g_{xx}	g_{yy}	w_{prp}^c	w_{pll}^c	$gib0^d$
TOL ^b	6.11 ^b	6.09 ^b	34.26 ^b	2.010 00 ^b	2.006 27 ^b	1.60 ^b	2.22 ^b	2.30 ^b
TOL	6.29	5.67	34.71	2.009 977	2.006 434	2.22	3.18	0.91
DMF	6.51	5.94	35.01	2.009 864	2.006 401	2.57	3.41	1.47
DBP	6.27	5.90	34.64	2.009 980	2.006 357	2.40	3.47	0.74
DOP	6.08	5.37	34.99	2.009 762	2.006 325	2.51	3.53	1.83

^a Regarding the minor differences in experimental values $g_{zz} = 2.0021$ has been kept during all simulations for simplicity. ^b Data for spin-labeled poly(styrene-co-acrylic acid) copolymer (SL-ST-AA) taken from ref 33. ^c Parameters characterizing axially symmetric inhomogeneous Lorentzian broadening of spectral lines. ^d Parameter characterizing Gaussian inhomogeneous broadening of spectral lines.

**Figure 2.** ESR spectra of the SL-ST-MA copolymer in DOP at given temperatures: experimental spectra, full lines; best-fitting simulated spectra, dotted lines.

simulated spectra fitting them best. Fits of similar quality have been reached in all four solvents. Some of the experimental spectra clearly indicate the presence of a small amount (less than 5% of total nitroxide concentration in the sample) of a much more mobile spin-label in the sample. We have frequently observed such a superposition in the ESR spectra of spin-labeled polymers in solutions, which is probably due to a slow detachment of some of the side chains through which the spin-label is bonded to the main chain. This results in the appearance of the free nitroxide spectrum. All such spectra have been analyzed using a two-site model.

The best fits of the experimental spectra, from both visual and statistical (e.g., correlation coefficients obtained from the NLSL program) points of view, were obtained when using the MOMD model with axially symmetric Brownian rotational diffusion (R_{prp} and R_{pll}) and with a local potential as a model for spin-label reorientation (site 1). The MOMD model, when applied to the system of nitroxide spin-labels attached via short side chains (tethers) to the polystyrene main chain in solution, implies a preferred orientation for the axis of internal rotation of each attached nitroxide label with respect to the polymer main chain, but there is an isotropic distribution of these preferred orientations in the macroscopic sample due to the random distribution of polymer orientations. The nature of the preferred orientational distribution within each polymer is determined by the shape of the ordering potential, which may

be varied by means of potential parameters c_0^2 , c_2^2 , c_0^4 etc., and optimized during the fitting process. The first three mentioned parameters were found to be sufficient in the present study. Site 2 spectra have been calculated assuming a simple axially symmetric Brownian rotational diffusion and practically the same values for **A** and **g** tensor components as for site 1. Only isotropic splitting constant has been used as one of the fitting parameters if needed; best-fit values in the limit 15.55 ± 0.05 G have been determined in all cases. The tractable basis set characterized by the parameters³⁵ $l_{\text{emx}} = 14$, $l_{\text{omx}} = 11$, $k_{\text{mx}} = 8$, and $i_{\text{pnmx}} = 2$ was found sufficient for both sites and was used for all calculations. We characterized all the presented fits as quite satisfactory despite some discrepancies due to the assumed possible presence of some distribution of mainly rotational parameters (R_{prp} and R_{pll}).

Arrhenius plots of the best-fit values determined for the rotational parameters R_S and R_I are given in Figure 3, and the data are presented in Table 2. The data for both parameters in all four solvents have been fitted by the equation

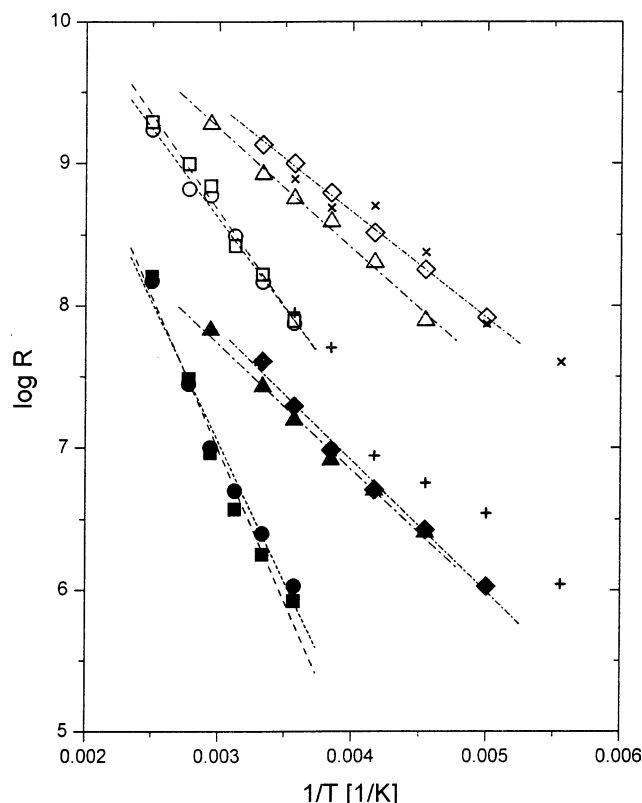
$$\log R_{S,I} = A'' - (E_{S,I}^{\text{exp}}/RT) \log e \quad (4)$$

which represents a linear dependence in $\log R$ vs $1/T$ coordinates and is analogous to eq 1 (A'' is independent of temperature). The best-fit parameters A'' and $E_{S,I}^{\text{exp}}$ together with values of corresponding correlation coefficients are given in Table 2 as well. Higher mobilities and lower activation energies $E_{S,I}^{\text{exp}}$ for both less viscous solvents (TOL and DMF) compared with both more viscous ones (DBP and DOP) follow from Figure 3. The figure has been completed with X-band data characterizing dynamics of the SL-ST-AA copolymer in a dilute toluene solution taken from our previous paper.³³ Comparing SL-ST-AA with SL-ST-MA, the absence of the methyl group in the polymer chain segment bearing nitroxide spin-label is probably responsible for a clearly visible higher segmental mobility in the former copolymer.

The best-fit values of the fitting parameters demonstrate general consistency of the model used. The angle β is solvent-dependent, slightly decreasing or being practically constant with increasing temperature in each of the solvents. The parameter c_0^2 characterizes the component of the ordering potential symmetric in the plane perpendicular to the direction of the preferred rotational tensor symmetry axis orientation specified by the angle β . This parameter increases with increasing temperature in all solvents used up to a maximum reached at intermediate temperatures at which a motionally narrowed character of the spectra begins to prevail, and it sharply decreases at higher temperatures. The parameter c_0^4 , which affects the shape of

Table 2. Temperature and Solvent Dependence of Rotational Parameters $R_{S,I}$ [s^{-1}], Parameters Characterizing the Best-Fit of the Temperature Dependence to Eq 4, and Apparent Activation Energies $E_{S,I}^{\text{exp}}$ [kJ/mol]

T [K]	TOL		DMF		DBP		DOP	
	$\log R_S$	$\log R_I$	$\log R_S$	$\log R_I$	$\log R_S$	$\log R_I$	$\log R_S$	$\log R_I$
200	6.0254	7.9150	-	-				
220	6.4256	8.2525	6.4070	7.8923				
240	6.7061	8.5126	6.7032	8.3029				
260	6.9822	8.7928	6.9145	8.5896				
280	7.2927	9.0010	7.1944	8.7543	6.0270	7.8732	5.9198	7.8911
300	7.6080	9.1321	7.4292	8.9242	6.3979	8.1668	6.2498	8.2173
320					6.6987	8.4903	6.5686	8.4192
340			7.8268	9.2998	7.0001	8.7748	6.9618	8.8402
360					7.4482	8.8192	7.4838	8.9946
400					8.1729	9.2351	8.2033	9.2890
A''	10.60	11.64	10.38	11.78	12.95	12.40	13.44	12.70
$E_{S,I}^{\text{exp}}$	17.7 ± 0.9	14.3 ± 0.3	16.9 ± 0.7	16.2 ± 0.7	37.8 ± 2.9	24.1 ± 1.4	41.2 ± 3.4	25.8 ± 1.5
corr	0.99515	0.99911	0.99643	0.99612	0.98833	0.99355	0.9869	0.9932

**Figure 3.** Arrhenius plots of rotational diffusion coefficients R_S (full symbols) and R_I (empty symbols) for the SL-ST-MA copolymer in four solvents (for solvent symbols, see Figure 1) and their best fits to eq 4. X-band data for the SL-ST-AA copolymer in toluene taken from ref 33 (R_S , +; R_I , x) are given for comparison.

ordering potential significantly, behaves in a similar way, reaching even negative values. The parameter c_2^2 characterizing rhombic distortion of the ordering potential keeps a relatively high value at temperatures at which the slow-motional character of the spectra prevails; at intermediate and higher temperatures, it sharply decreases toward zero. For the nitroxide spin-label chemically attached to polymer chains in solution, the conclusions presented above generally confirm the importance of microscopic ordering for the dynamics resulting in slow-motional ESR spectra and its decreasing effect on the dynamics in the motional narrowing region. Information on the shape of ordering potential, characterized by the parameters c_0^2 and c_2^2 , and on its dependence on polymer structure, solvent, and temperature is expected to bring detailed insight into local

dynamic of polymers in solution, in particular into distribution of orientations of axis for internal rotation. A relatively low amount of available data and, in particular, low sensitivity of spectral line shapes to some of the ordering parameters prevents us from discussing relations between the shape of the ordering potential and some structural aspects in more details at present. The values of ordering parameters c_0^2 and c_2^2 determined when analyzing ESR spectra of the SL-ST-MA copolymer fall in the same range as the values determined when analyzing ESR spectra of the SL-ST-AA copolymer given in the previous paper³³ where the different "seeing" of polymer dynamics by X-band and high-field (250 GHz) ESR has been discussed.

The temperature dependence of viscosity of the solvents used does not exhibit Arrhenius behavior even in the temperature ranges studied. This follows from Figure 1, which clearly shows nonlinearity of the plots in $\log \eta$ vs $1/T$ coordinates. As a consequence, the activation energy of the viscous flow of the solvent, E_η , cannot be a relevant parameter for further discussion. For this reason, we have used the approach introduced by Glowinkowski et al.¹⁸ Equation 1 can be rewritten in the form

$$\log R_S = A''' - \alpha \log [\eta(T)] - (E_a/RT) \log e \quad (5)$$

where A''' is independent of temperature and viscosity.

In the inset of Figure 4, we have plotted $\log R_S$ vs $\log \eta$ at three temperatures at which measurements at least in three of four solvents have been performed. At a constant temperature, the slopes of these plots determine the values of the coefficient α , as follows from eq 5. Linear fits to the presented data have afforded the value $\alpha = 0.73 \pm 0.02$ at all three temperatures. Equation 1 can be rewritten also in the form

$$\log (R_S[\eta(T)]^\alpha) = A''' - (E_a/RT) \log e \quad (6)$$

Finally, we have plotted $\log(R_S\eta^{0.73})$ vs $1/T$ in Figure 4. The linear fit to the data characterized by satisfactory correlation coefficient 0.9712 has yielded the value $E_a = 10.5 \pm 0.6$ kJ/mol for the solvent-independent height of potential barrier for local dynamics of polystyrene chains. Four points indicated in Figure 4 have been excluded from the data set before performing the fit. In the case of DOP and DBP high-temperature data, the reason consists of the fact that the corresponding ESR spectra could not be analyzed using a two site-model because their line shapes were practically insensitive to the site 2 parameters. The one site model fit cannot

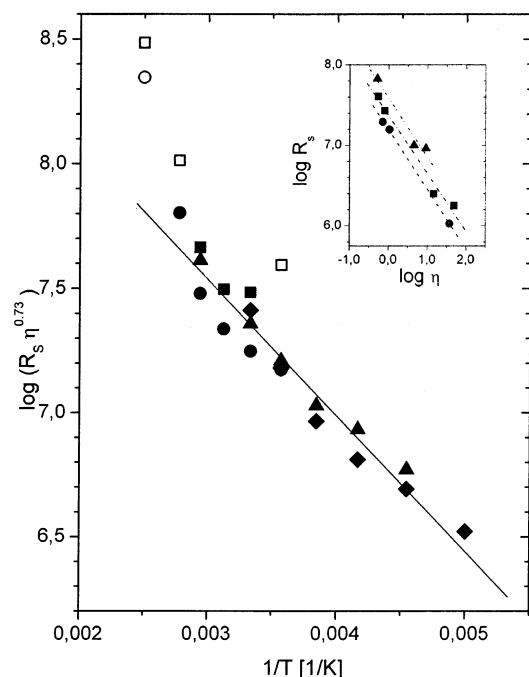


Figure 4. Arrhenius plot of reduced diffusion coefficient $R_S \eta^{0.73}$ (for solvent symbols, see Figure 1). The line is the best fit by eq 6, and its slope gives $E_a = 10.5 \pm 0.6$ kJ/mol. The points excluded from the fit are given by empty symbols. Log R_S vs log dependence at 280 (\blacktriangle), 300 (\blacksquare), and 340 K (\bullet) is given in the inset. At all temperatures, the slope gives $\alpha = 0.73 \pm 0.02$.

give parameters consistent with the two-site one due to disregarding the second-site contribution. The value determined in DOP at 280 K was excluded because of increased error in its determination due to a low sensitivity of the line shape of the corresponding ESR spectrum to the R_{prp} parameter. The error in determination of R_S parameters by fitting all other ESR spectra has been estimated at 10%.

Conclusions

A styrene copolymer with methacrylic acid containing less than 5 mol % of spin-labeled methacrylic acid units distributed randomly along the main chain was synthesized. ESR spectra of the copolymer were measured at X-band (9 GHz) in dilute solutions (ca. 1 wt %) over a broad temperature range in four solvents differing in thermodynamic quality, viscosity, and activation energy of viscous flow. The temperature dependence of the parameter R_S , characterizing the local dynamics in polystyrene chains, and of the other parameters characterizing dynamics in the copolymer studied were determined by fitting experimental ESR spectra to the MOMD model. Unlike the authors of papers published so far, we have concluded that the SL-ST-MA copolymer in the solvents used, regardless of their thermodynamic quality, exhibits non-Kramers' behavior characterized by parameter $\alpha = 0.73 \pm 0.02$ and by the height of the potential barrier for local conformational transitions $E_a = 10.5 \pm 0.6$ kJ/mol. The value agrees with the value published by Waldow et al.² for good solvents ($E_a = 11 \pm 3$ kJ/mol) within the given error limits. The difference between the value of parameter α determined in the present paper and the value determined by Waldow et al.² using the anthracene chromophore bonded inside the polystyrene chain and the fluorescence depolarization technique ($\alpha = 0.9$) is minor.

Nevertheless, a higher α value has been found by the fluorescence depolarization technique in the presence of bulky chromophore label² than by ESR in the presence of the nitroxide spin-label affecting the chain geometry to a small extent. A similar case was observed with polyisoprene when comparing values determined by the fluorescence depolarization technique⁴ and no-label NMR¹⁸ (0.75 and 0.41, respectively). When comparing the three mentioned techniques used for characterization of local segmental dynamics in polymers, only the NMR technique does not require the presence of any label affecting the chain dynamics; on the other side, its applicability requires appearance of suitable lines in the NMR spectrum of the polymer (¹³C enrichment is frequently needed). The presence of bulky chromophore label bonded inside the main chain required when applying fluorescence technique affects both main chain conformation and dynamics in the vicinity of the "signal" group significantly. The ESR technique requires the presence of the spin-label that is usually attached to a short side chain; the volume and structure of the spin-label bearing chain unit are usually very similar to the volume and structure of the main chain units. Information on the local main chain dynamics is extracted from the parameters characterizing anisotropic rotational diffusion of the label. The ESR spin-label technique is applicable to polymer systems (copolymers, gels) regardless of their complicated chemical structure, providing that a suitable way of spin-label attachment to them is found.

Acknowledgment. This research was supported by the Grant Agency of the Academy of Sciences of the Czech Republic (Project A4050804) and by the Academy of Sciences of the Czech Republic (Project AVOZ4050913). We thank Dr. P. Štěpánek (IMC Prague) for stimulating discussions.

References and Notes

- (1) Ediger, M. D. *Annu. Rev. Phys. Chem.* **1991**, *42*, 225.
- (2) Waldow, D. A.; Ediger, M. D.; Yamaguchi, Y.; Matsushita, Y.; Noda, I. *Macromolecules* **1991**, *24*, 3147.
- (3) Johnson, B. S.; Ediger, M. D.; Yamaguchi, Y.; Matsushita, Y.; Noda, I. *Polymer* **1992**, *33*, 3916.
- (4) Adolf, D. B.; Ediger, M. D.; Kitano, T.; Ito, K. *Macromolecules* **1992**, *25*, 867.
- (5) Johnson, B. S.; Ediger, M. D.; Kitano, T.; Ito, K. *Macromolecules* **1992**, *25*, 873.
- (6) Yokotsuka, S.; Okada, Y.; Tojo, Y.; Sasaki, T.; Yamamoto, M. *Polym. J.* **1991**, *23*, 95.
- (7) Ono, K.; Okada, Y.; Yokotsuka, S.; Sasaki, T.; Yamamoto, M. *Macromolecules* **1994**, *27*, 6482.
- (8) Ono, K.; Ueda, K.; Yamamoto, M. *Polym. J.* **1994**, *26*, 1345.
- (9) Ono, K.; Ueda, K.; Sasaki, T.; Murase, S.; Yamamoto, M. *Macromolecules* **1996**, *29*, 1584.
- (10) Horinaka, J.; Amano, S.; Funada, H.; Ito, S.; Yamamoto, M. *Macromolecules* **1998**, *31*, 1197.
- (11) Horinaka, J.; Aoki, H.; Ito, S.; Yamamoto, M. *Polym. J.* **1999**, *31*, 172.
- (12) Horinaka, J.; Maruta, M.; Ito, S.; Yamamoto, M. *Macromolecules* **1999**, *32*, 1134.
- (13) Horinaka, J.; Ito, S.; Yamamoto, M.; Tsujii, Y.; Matsuda, T. *Macromolecules* **1999**, *32*, 2274.
- (14) Soutar, I.; Swanson, L.; Christensen, R. L.; Drake, R. C.; Phillips, D. *Macromolecules* **1996**, *29*, 4931.
- (15) Heatley, F.; Begum, A. *Polymer* **1976**, *17*, 399.
- (16) Heatley, F.; Wood, B. *Polymer* **1978**, *19*, 1405.
- (17) Gronski, W.; Schäfer, T.; Peter, R. *Polym. Bull. (Berlin)* **1979**, *1*, 319.
- (18) Glowinkowski, S.; Gisser, D. J.; Ediger, M. D. *Macromolecules* **1990**, *23*, 3520.
- (19) Gisser, D. J.; Glowinkowski, S.; Ediger, M. D. *Macromolecules* **1991**, *24*, 4270.
- (20) Gisser, D. J.; Ediger, M. D. *Macromolecules* **1992**, *25*, 1284.

- (21) Spyros, A.; Dais, P.; Heatley, F. *Macromolecules* **1994**, *27*, 6207.
- (22) Tylianakis, E. I.; Dais, P.; Heatley, F. *J. Polym. Sci., Part B: Polym. Phys.* **1997**, *35*, 317.
- (23) Karali, A.; Dais, P.; Heatley, F. *Macromolecules* **2000**, *33*, 5524.
- (24) Adolf, D. B.; Ediger, M. D. *Macromolecules* **1991**, *24*, 5834.
- (25) Adolf, D. B.; Ediger, M. D. *Macromolecules* **1992**, *25*, 1074.
- (26) Moe, N. M.; Ediger, M. D. *Macromolecules* **1995**, *28*, 2329.
- (27) Kramers, H. A. *Physica* **1940**, *7*, 284.
- (28) Courtney, S. H.; Fleming, G. R. *J. Chem. Phys.* **1985**, *83*, 215.
- (29) Helfand, E. *J. Chem. Phys.* **1971**, *54*, 4651.
- (30) Pilař, J.; Labský, J. *J. Phys. Chem.* **1986**, *90*, 6038.
- (31) Pilař, J.; Labský, J. *Macromolecules* **1991**, *24*, 4188.
- (32) Pilař, J.; Labský, J. *Macromolecules* **1994**, *27*, 3977.
- (33) Pilař, J.; Labský, J.; Marek, A.; Budil, D. E.; Earle, K. A.; Freed, J. H. *Macromolecules* **2000**, *33*, 4438.
- (34) Schneider, D. J.; Freed, J. H. In *Biological Magnetic Resonance*; Berliner, L. J., Reuben, J., Eds.; Plenum: New York, 1989; Vol. 8, p 1.
- (35) Budil, D. E.; Lee, S.; Saxena, S.; Freed, J. H. *J. Magn. Reson., Ser. A* **1996**, *120*, 155.
- (36) Bullock, A. T.; Cameron, G. G.; Smith, P. M. *J. Chem. Soc., Faraday Trans. 2* **1974**, *70*, 1202 and references therein.
- (37) Meirovitch, E.; Nayeem, A.; Freed, J. H. *J. Phys. Chem.* **1984**, *88*, 3454.
- (38) Labský, J.; Pilař, J.; Lövy, J. *J. Magn. Reson.* **1980**, *37*, 515.
- (39) *International Critical Tables*; Washburn, E. W., West, C. J., Dorsey, N. E., Ring, M. D., Eds.; McGraw-Hill Book Co., Inc.: New York, 1930; Vol. VII, p 218.
- (40) Barlow, A. J.; Lamb, J.; Matheson, A. J. *Proc. R. Soc. London, Ser. A* **1966**, *292*, 322.
- (41) *CRC Handbook of Chemistry and Physics*, 76th ed.; CRC Press: Boca Raton, FL, 1995–1996; pp 6–245.
- (42) Guttman, F.; Simons, L. *J. Appl. Phys.* **1952**, *23*, 977.
- (43) Štěpánek, P. Ph.D. Thesis, Institute of Macromolecular Chemistry, Prague, 1981.
- (44) Monsanto Co. Publications No. 1537 and No. 1530.
- (45) Marchetti, A.; Preti, C.; Tagliazucchi, M.; Tassi, L.; Tosi, G. *J. Chem. Eng. Data* **1991**, *36*, 360.
- (46) Berry, G. C. *J. Chem. Phys.* **1967**, *46*, 1338.
- (47) Štěpánek, P.; Koňák, Č.; Sedláček, B. *Macromolecules* **1982**, *15*, 1214.
- (48) Moore, R. S.; McSkimin, H. J.; Gieniewski, C.; Andreath, P., Jr. *J. Chem. Phys.* **1967**, *43*, 3; **1969**, *50*, 5088.
- (49) Candau, S. J.; Butler, I.; King, T. A. *Polymer* **1983**, *24*, 1601.
- (50) Štěpánek, P.; Koňák, Č. *Collect. Czech. Chem. Commun.* **1987**, *52*, 1246.

MA025687H